Application Note

Cell Analysis

Agilent

Trusted Answers

AI-Enabled Cell Morphology Profiling Using Automated Imaging and Analysis

An Agilent BioTek workflow with integrated Cellpose-powered segmentation and quantitative morphology profiling to enhance EMT characterization

Authors

Ernest Heimsath, PhD,
Rebecca Mongeon, PhD,
Joe Clayton, PhD,
Agilent Technologies, Inc.

Antony Wood, PhD
Cell Signaling Technology

Abstract

The epithelial-to-mesenchymal transition (EMT) is a dynamic cellular differentiation process central to development, tissue remodeling, and cancer progression. Canonical EMT signaling through the TGF-β/SMAD axis induces coordinated biochemical, transcriptional, and phenotypic changes that are commonly evaluated using phospho-SMAD signaling events and downstream transcription factor expression. While antibody-based imaging readouts provide highly specific and quantitative insights into pathway activation, EMT is fundamentally accompanied by changes in cell shape, cytoskeletal organization, and population-level morphology that have historically been more difficult to quantify in a high-throughput and reproducible manner.

In this application note, we demonstrate how recent advances in AI-based image segmentation enable robust, quantitative morphological profiling that complements established antibody-based analyses. Images acquired with the Agilent BioTek Cytation C10 confocal imaging reader were analyzed using the Agilent BioTek Gen5 AI cell identification module with integrated Cellpose-SAM foundational model. Interpretable, single-cell morphology features were extracted from phalloidin- and DAPI-stained images acquired as part of a typical EMT imaging workflow across a TGF-beta dose-response series. Morphology-derived metrics exhibited clear, concentration-dependent responses that were consistent with changes observed in the expression of canonical EMT markers. Integration of AI-enabled morphological analysis with traditional immunofluorescence workflows expands EMT assessment by combining quantitative phenotypic readouts with validated antibody-based measurements.

Introduction

The EMT is a highly coordinated cellular differentiation program in which epithelial cells progressively lose apico-basal polarity and intercellular adhesion while acquiring mesenchymal characteristics such as increased motility and cytoskeletal reorganization.[1–3] EMT plays essential roles in embryonic development and tissue repair, and its dysregulation has been implicated in cancer invasion and metastasis.[2, 3] Central to EMT induction in many epithelial systems is signaling through the TGF-β superfamily, which activates canonical SMAD dependent pathways and regulates the expression of EMT associated transcription factors, including HMGA2, ZEB1, and Slug.[1, 2, 4, 5, 6]

Antibody-based methods targeting phosphorylated SMAD proteins and EMT-associated transcription factors have become widely adopted tools for quantitatively assessing pathway activation and downstream responses in both two and three dimensional (2D and 3D) cellular models.[4, 5, 7] These approaches provide specificity, sensitivity, and direct biological interpretability, making them foundational to EMT research and drug discovery workflows.

In parallel with these molecular and biochemical changes, EMT is accompanied by pronounced alterations in cell morphology, actin organization, and population-level architectural features.[2, 3] While such phenotypic changes are frequently observed qualitatively, their quantitative analysis has historically been limited by challenges in accurate cell segmentation and feature extraction, particularly in dense epithelial monolayers.

Recent advances in AI-based image analysis, including generalist segmentation approaches such as Cellpose, now enable robust and reproducible delineation of individual cells and nuclei across a wide range of imaging conditions.[8, 9] These developments make it feasible to quantitatively assess EMT-associated morphological changes at single-cell and population scales, using standard cellular and nuclear counterstains already incorporated into many immunofluorescence workflows.

In this study, AI-enabled cell morphology analysis was incorporated into an established high-throughput EMT assay. Images were acquired using the Cytation C10 confocal imaging reader and analyzed with the BioTek Gen5 AI cell identification module featuring integrated Cellpose-powered segmentation. This approach combines established EMT biomarker analysis with single-cell morphology profiling to provide a more comprehensive, multiparametric assessment of cell state transitions.

Experimental

Materials

Reagents

Unless otherwise noted, chemicals were sourced from Sigma-Aldrich (Burlington, MA, USA). Human recombinant TGF-β1 and IL-1β were obtained from Cell Signaling Technology (CST; Danvers, MA, USA; part numbers 75362 and 54059, respectively). Antibodies directed against EMT-associated transcription factors were supplied by CST and validated for immunofluorescence applications, including HMGA2 (D1A7) (part number 8179), ZEB1 (E3G6Y) XP Rabbit mAb (part number 70512), and Slug (C18G7) Rabbit mAb (part number 9585).

Alexa Fluor 488-conjugated phalloidin (part number A12379) and Hoechst 34580 nuclear stain (part number H21486) were obtained from Thermo Fisher Scientific (Waltham, MA, USA). A CF633-conjugated goat anti-rabbit secondary antibody was purchased from Biotium (Fremont, CA, USA; part number 20131). Fibronectin was obtained from Sigma-Aldrich (part number F1141).

Cell culture

A549 human lung epithelial carcinoma cells were purchased from ATCC (Manassas, VA, USA; part number CC-185) and cultured in Advanced DMEM (Gibco; part number 12491) supplemented with 10% fetal bovine serum (Gibco; part number A5256501) and penicillin/streptomycin/glutamine (Gibco; part number 10378016). Cells were maintained under standard culture conditions at 37 °C in a humidified atmosphere containing 5% CO_2.

For imaging-based assays, cells were plated into Agilent 96-well imaging microplates (part number 204626-100) precoated with 10 µg/mL fibronectin to promote uniform cell adhesion and monolayer formation.

Instrumentation

Imaging was performed using the Cytation C10 configured with a 60 µm spinning disk. The instrument was equipped with a 20x plan fluorite objective with NA 0.45 (part number 1220517), and the following accessories: confocal DAPI filter cube (part number 1945103), confocal GFP filter cube (part number 1945104), confocal CY5 filter cube (part number 1945100), and laser autofocus cube (part number 1225010).

Image acquisition and environmental conditions were managed with the Agilent BioTek Gen5 software for imaging & microscopy.

Methods

Cell culture and treatment

Cultured A549 cells were regularly passaged at ~ 80% confluency before experimentation. Cells were harvested and plated at ~ 15,000 cells per well in 96-well microplates. After full attachment (overnight), complete media was removed and cells were serum-starved for approximately 18 hours in Advanced DMEM lacking fetal bovine serum (FBS). Cells were then treated with recombinant human TGF-β1 across a range of concentrations, as well as 10 ng/mL IL-1β for 48 hours at 37 °C to induce EMT-associated signaling responses. Vehicle-treated cells served as negative controls.

Sample preparation

Following treatment, cells were fixed with 4% paraformaldehyde for 10 minutes at room temperature. Fixed cells were then washed with DPBS and permeabilized with DPBS solution containing 0.5% Triton X-100 and 5% bovine serum albumin (BSA) to reduce nonspecific antibody binding.

Primary antibodies targeting EMT-associated transcription factors were incubated overnight at 4 °C according to the manufacturer's recommendations. After washing, cells were incubated with the fluorescently labeled secondary antibody in the presence of Hoechst 34580 and Alexa Fluor 488-conjugated phalloidin to enable simultaneous visualization of nuclei and F-actin structures.

Automated image capture and processing

Fluorescence images were automatically acquired using the Cytation C10 confocal imaging reader and Gen5 software. Multichannel fluorescence images were collected in a 16-image Z-stack at 2.0 µm intervals across DAPI (nuclear stain), GFP (phalloidin), and CY5 (antibody) channels. Laser autofocus was used to maintain focus across the 96-well microplate and consistent exposure and acquisition settings were applied across all treatment conditions.

Acquired images were Z-projected using a maximum signal algorithm, followed by background flattening with a rolling ball algorithm whose size was related to the expected object size in each channel. Specifically, the phalloidin (GFP) imaging channel was processed with default rolling ball settings (126 µm) while channels containing nuclear localized signals (DAPI and CY5 antibody) were processed with 30 µm rolling ball.

Image and data analysis

AI-based segmentation was performed using the Agilent BioTek Gen5 AI cell identification module with the integrated Cellpose-SAM v4.1.1 segmentation engine. Segmentation was performed using the cpsam pretrained model within the Cellular Analysis workflow. Cellpose-SAM is a generalist cell segmentation approach designed to identify cellular and nuclear objects across diverse microscopy images with minimal assay-specific optimization. For Cellpose-SAM segmentation in the Cellular Analysis workflow, DAPI images were first passed for nuclear detection as primary objects. Next, DAPI and phalloidin staining channels were passed together for Cellpose-SAM segmentation in a secondary mask detection step to generate whole-cell masks for downstream morphology measurements. Nuclear masks and cellular masks were associated in the BioTek Gen5 AI cell identification module using default settings. For traditional intensity-based analysis, the DAPI channel was first segmented in a primary object detection step to identify nuclei. Next, a secondary mask for whole-cell segmentation was created from the boundary of the primary nuclear mask using threshold-based propagation in the GFP channel. Threshold-based detection used default settings with the following adjustments: the secondary mask threshold value in the GFP channel was reduced to 3000 and image smoothing strength increased to 7. Antibody-based transcription factor signal quantification was derived from Cellpose-SAM-based nuclear segmentation masks.

Quantitative metrics derived from segmentation mask analysis were aggregated at the well level and mean well values were plotted as a function of TGF-β concentration. Dose-response relationships were fitted with four-parameter logistic curves to establish IC/EC_{50} values. Z-scores were calculated in Gen5 software using the following formula:

$$Z = \frac{(X - (CTL1)}{SD(CTL1)}$$

Results and discussion

AI-enabled segmentation supports robust single-cell morphological analysis

Induction of EMT in cultured epithelial monolayers is an established model for microscopy-based analysis of cellular protein expression and morphology. However, accurate segmentation in dense cultures can be challenging with traditional intensity-based approaches. AI models offer an alternative approach for accurate cell segmentation.

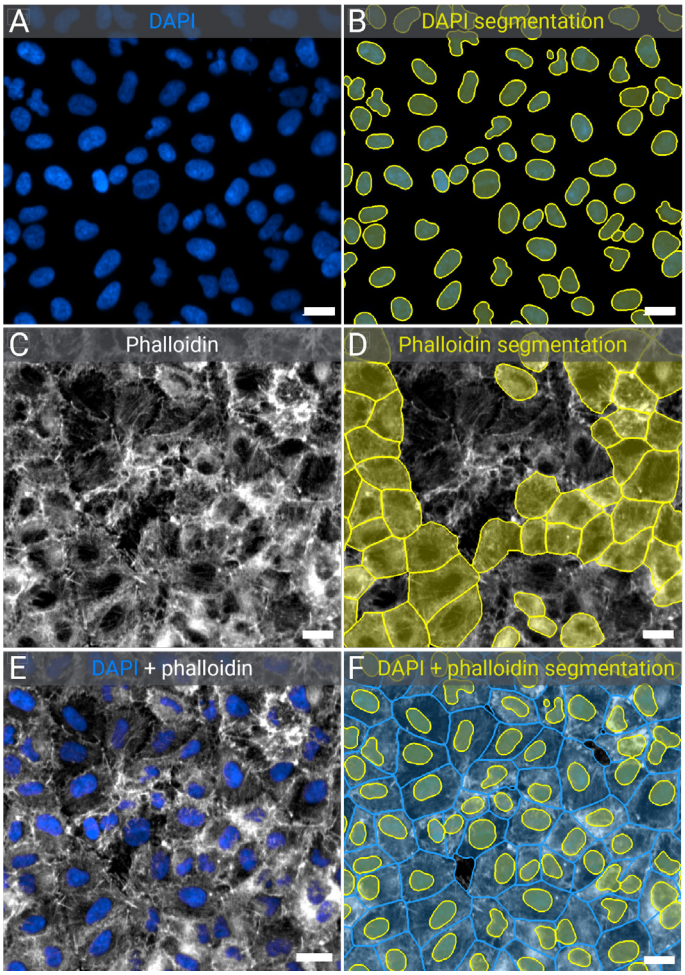

Figure 1. AI-based segmentation enables quantitative single-cell morphological analysis across dense monolayers. Representative A549 fluorescence images stained with DAPI and phalloidin are shown alongside Cellpose-SAM-generated segmentation masks. (A and B) Cellpose-SAM accurately segments nuclei from the DAPI channel. (C and D) Phalloidin signal alone is insufficient for accurate whole-cell segmentation. (E and F) Combined DAPI and phalloidin inputs enable accurate Cellpose-SAM whole-cell segmentation. Scale bars, 20 µm.

Figure 1 shows a typical epithelial monolayer of cultured A549 cells that were fixed and stained with DAPI and phalloidin and imaged at 20x magnification with the Cytation C10 confocal imaging reader to visualize nuclear DNA and the actin cytoskeleton. This staining combination is a standard and informative approach that reports on both nuclear and cellular morphology, including the cytoskeletal arrangements associated with EMT. However, the variable distribution and intensity of phalloidin staining presents challenges for accurate boundary determination with traditional intensity-based methods. Here, we investigated whether Cellpose-SAM could generate segmentation masks from these staining conditions that were sufficient for quantitative morphology analysis in EMT applications.

Analysis of the nuclear DAPI channel alone (Figure 1A) with Cellpose-SAM and default parameter settings yields accurate nuclear segmentation (Figure 1B). Analysis of the phalloidin channel alone (Figure 1C) with Cellpose-SAM only yielded accurate cell identification for a fraction of the cells in the image. However, passing both the DAPI and phalloidin channels together to Cellpose-SAM (Figure 1E) yielded a clear improvement in cell segmentation accuracy based on image inspection. Further minor improvements to segmentation were also observed when increasing the flow threshold parameter from default value of 0.4 to 0.6.

The objective of this application note was to determine whether Cellpose-SAM segmentation performance in a standard DAPI/phalloidin immunofluorescence workflow was sufficient to support biologically meaningful EMT morphology measurements through interpretable feature extraction. The application note was not designed to benchmark Cellpose-SAM segmentation accuracy exhaustively or to optimize staining and segmentation conditions across multiple labeling strategies.

Cellpose-SAM was trained and tested with fluorescence images that included nuclear labels and membrane or cytoplasmic dyes that label the whole cell region.[9] Regardless, the broadly generalizing nature of Cellpose-SAM may help explain its ability to discriminate cell boundaries from phalloidin staining. In this workflow, Cellpose-SAM segmentation was sufficiently robust to support high-throughput, image-based quantitative morphology analysis in parallel with antibody-based expression analysis.

Morphological remodeling following TGF-β treatment is resolved by AI-based segmentation

AI-based whole-cell segmentation of nuclear and phalloidin staining was used to evaluate fixed cultures of A549 cells treated with TGF-β to induce EMT morphology and expression changes. Visual inspection of cells under control and TGF-β treatment (Figure 2) demonstrated a shift from cuboidal-like epithelial shape with relatively diffuse actin cytoskeleton (Figure 2A) to substantially elongated cells with cytoskeletal rearrangement and actin stress fiber formation (Figure 2D).

AI-based segmentation of the DAPI and phalloidin staining enabled comparison of morphology parameters derived from the whole-cell masks. Both untreated (Figure 2B) and EMT-induced cells (Figure 2E) were successfully segmented with AI-based analysis. In contrast, traditional intensity-based segmentation of these same images struggled to properly identify cell boundaries, with inaccuracies particularly apparent for TGF-β-treated cells (Figures 2C and F).

For intensity-based analysis, primary masks were first generated from nuclei identified in the DAPI channel, which were then used as seed objects to propagate cell masks within the phalloidin channel using a threshold-based approach. However, phalloidin staining in epithelial monolayers does not consistently provide the smooth intracellular intensity gradients or well-defined intensity minima between cells required for reliable threshold-based detection. As a result, the masks shown in Figures 2C and F are driven primarily by radial expansion from the nuclear seeds rather than detected cell boundaries, yielding only an approximate representation of cell shape.

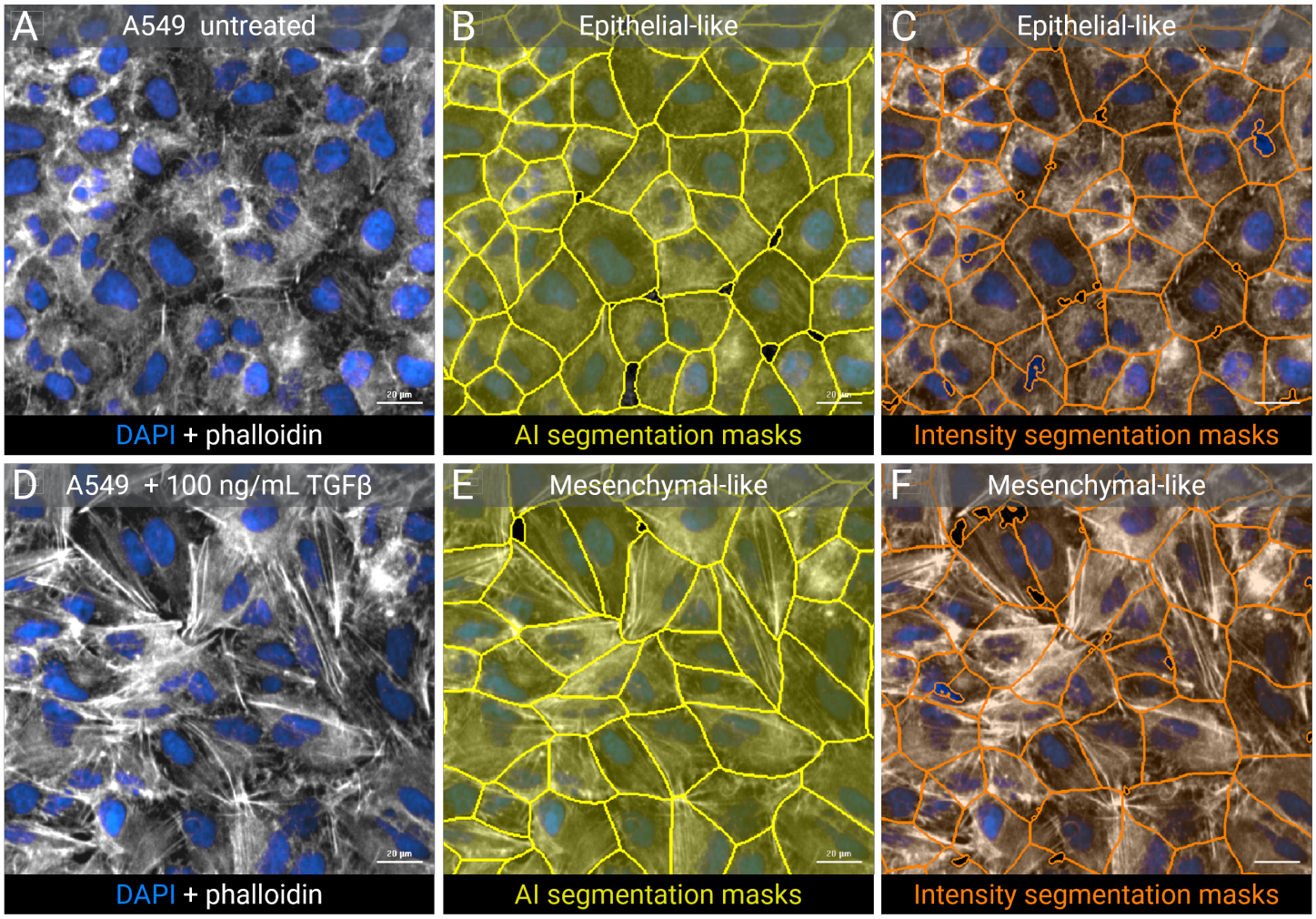

Figure 2. AI-based segmentation resolves TGF-β-induced morphological remodeling. (A) Untreated A549 monolayers stained with DAPI and phalloidin show epithelial-like cuboidal morphology. (B) Cellpose-SAM segmentation accurately resolves cell boundaries in untreated cultures. (C) Traditional intensity-based analysis of the same image shown in panel (A) poorly approximates intercellular boundaries. (D) TGF-β-treated A549 cultures show cytoskeletal rearrangement and elongation consistent with transition toward a mesenchymal phenotype. (E) Cellpose-SAM segmentation accurately resolves cell boundaries in treated cultures. (F) Traditional intensity-based analysis of the same image shown in panel (D) relies on radial expansion from nuclear seeds, which becomes a poor approximation of true cell morphology as cells elongate. Scale bars, 20 µm.

Morphological features exhibit dose-dependent responses to TGF-β stimulation

Agilent BioTek Gen5 software generates intuitive, interpretable cellular morphology measurements of cell segmentation masks for both intensity- and AI-based segmentation (Figure 3). Cell-level morphology metrics were extracted and evaluated for A549 cell cultures across the TGF-β dose-response series.

For the segmentation derived from Cellpose-SAM (Figures 3A to C), each of the morphology metrics, including aspect ratio, form factor and solidity, exhibited a concentration-dependent shift consistent with EMT progression. Of these shape metrics, aspect ratio showed the most pronounced decrease with increasing TGF-β concentration, reflecting elongation of cells during the epithelial-to-mesenchymal transition.

Form factor and solidity metrics also demonstrated smaller but measurable changes across the dose range, capturing alterations in boundary complexity and cytoskeletal organization associated with EMT.

In contrast, morphology metrics derived from intensity-based segmentation of the same dataset showed increased variability without a clear dose-dependent relationship with TGF-β concentration. For this application, the inaccuracies associated with approximate masks render intensity-based approaches insufficient for EMT morphology analysis.

Together, these results demonstrate that accurate cell boundary segmentation is critical for reliable extraction of morphology-based features and that AI-based approaches enable robust quantification of EMT-associated phenotypic changes.

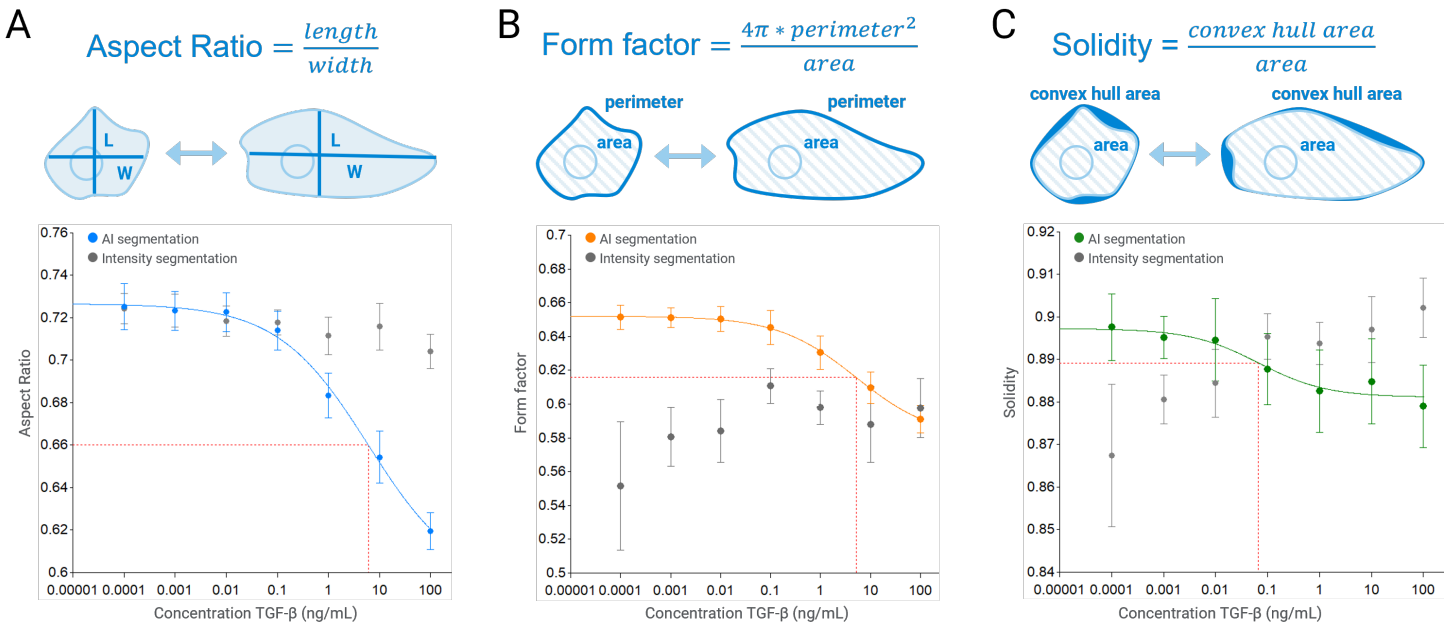

Figure 3. Agilent BioTek Gen5 software morphology metrics quantify TGF-β-induced changes from AI-generated segmentation masks. Morphology metrics were calculated from segmentation masks generated using Cellpose-SAM segmentation or traditional intensity-based thresholding. (A) Aspect ratio calculation and dose-response analysis show that Cellpose-SAM segmentation captures TGF-β-induced cell elongation more effectively than threshold-based segmentation. (B) Form factor calculation and dose-response analysis show morphology changes consistent with EMT-associated elongation. (C) Solidity calculation and dose-response analysis capture EMT-associated changes in cell shape and boundary complexity. For each metric, AI- and threshold-based segmentation results are compared across the TGF-β dose-response series.

Antibody-based EMT markers confirm morphology-derived phenotypic responses

To assess how morphology-based measurements relate to established molecular markers of EMT, morphology-derived metrics were compared with antibody-based quantification of EMT-associated transcription factors, including HMGA2, ZEB1, and Slug (Figure 4).

Z score analysis of morphology features identified cell aspect ratio as a particularly responsive metric across the TGF-β dose range (Figure 4A). Among the shape measurements evaluated, aspect ratio showed the most consistent and pronounced decrease relative to untreated controls as TGF-β concentration increased, reflecting progressive cell elongation during EMT. Cellular form factor also changed in a direction consistent with EMT progression, but the response was smaller in magnitude and reached clear separation from control values only at the highest TGF-β concentrations tested.

When compared directly (Figure 4B), morphology-derived aspect ratio exhibited a concentration-dependent profile that paralleled the induction of EMT-associated transcription factors. The fitted half maximal response values were 14.6 ng/mL for HMGA2, 2.8 ng/mL for ZEB1, 6.2 ng/mL for Slug, and 4.7 ng/mL for cell aspect ratio. These results indicated that aspect ratio provides a morphology-based readout with sensitivity comparable to selected antibody-based EMT markers, responding over a similar concentration range and with similar response magnitude.

While antibody-based measurements provide specific insight into transcriptional regulation downstream of TGF β signaling, morphology based metrics reflect the integrated phenotypic outcome of these molecular events. The combination of these readouts therefore provides complementary perspectives on EMT progression, linking pathway activation to observable changes in cellular structure and organization.

Collectively, these data demonstrate that AI-enabled morphological profiling can be readily integrated with established immunofluorescence workflows to enhance interpretation of EMT-associated responses without altering existing assay designs.

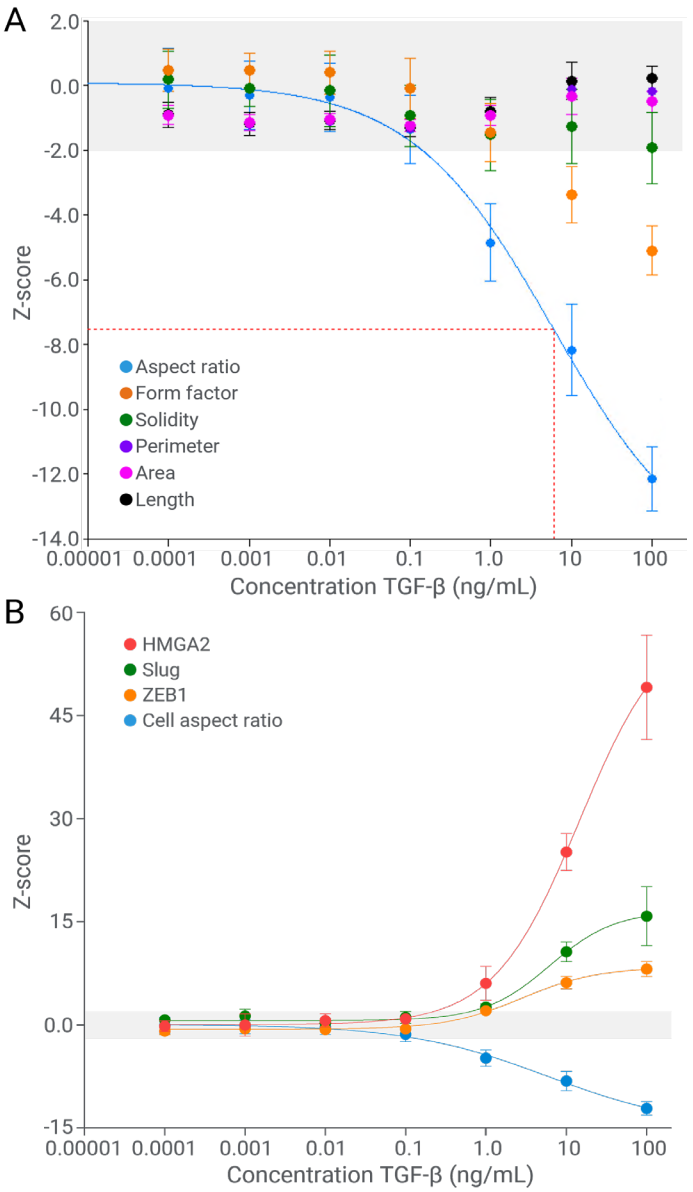

Figure 4. Morphological and antibody-based readouts provide complementary views of EMT. (A) Z scores for morphology metrics are plotted as a function of TGF-β concentration. Data points represent mean ± standard deviation from n = 12 replicate wells, with four-parameter logistic fits shown as solid lines. The gray region indicates the −2 to 2 Z score range used as the control-range threshold. Aspect ratio, calculated as length/width, showed the strongest morphology-based response, while form factor exceeded the ± 2 Z score threshold at two concentrations with a smaller overall response. (B) Morphology dose-response profiles are compared with antibody-based measurements of EMT-associated transcription factors HMGA2, ZEB1, and Slug. Antibody signal data points represent mean ± standard deviation from n = 3 replicate wells, with four-parameter logistic fits shown as solid lines. Half maximal response values from the fitted curves were 14.6 ng/mL for HMGA2, 2.8 ng/mL for ZEB1, 6.2 ng/mL, and 4.7 ng/mL for cell aspect ratio.

Conclusions

This study demonstrates that AI-enabled morphology analysis provides an efficient and sensitive workflow for quantitative EMT assessment in a TGF-β-induced model. Importantly, the morphology responses occurred over a similar concentration range and relative magnitude compared to antibody-based analysis of validated EMT-associated transcription factor expression. These results support morphology-based profiling as a sensitive, biologically meaningful phenotypic readout that can complement and extend antibody-based EMT analysis.

Using the integrated Cellpose-SAM analysis in the Agilent BioTek Gen5 AI cell identification module, routine cytoskeletal and nuclear staining workflows supported whole-cell segmentation that was sufficiently robust for extracting interpretable morphology features from dense A549 epithelial cultures. Morphology-derived metrics exhibited clear, concentration-dependent responses to TGF-β stimulation that aligned with established EMT-associated phenotypic changes and were not reliably captured using conventional intensity-based segmentation. From a workflow perspective, implementation within an automated imaging solution that integrates Cellpose-SAM segmentation enables scalable, reproducible high-throughput analysis and multiparametric insights from a single assay design. Moreover, this workflow links molecular marker expression with downstream changes in cell shape and cytoskeletal organization while preserving compatibility with established immunofluorescence protocols.

The AI-enabled workflow presented in this application note extends the analytical power of imaging-based approaches and provides a practical framework for robust phenotypic screening and more comprehensive characterization of cellular responses in cancer research and drug discovery applications.

References

1. Aigner, K.; Dampier, B.; Descovich, L.; Mikula, M.; Sultan, A.; Schreiber, M.; Mikulits, W.; Brabletz, T.; Strand, D.; Obrist, P.; Sommergruber, W.; Schweifer, N.; Wernitznig, A.; Beug, H.; Foisner, R.; Eger, A. The Transcription Factor ZEB1 (δEF1) Promotes Tumour Cell Differentiation by Repressing Master Regulators of Epithelial Polarity. *Oncogene* **2007**, *26*, 6979–6988. DOI: 10.1038/sj.onc.1210508
2. Peinado, H.; Olmeda, D.; Cano, A. Snail, Zeb and bHLH Factors in Tumour Progression: An Alliance Against the Epithelial Phenotype? *Nat. Rev. Cancer* **2007**, *7*, 415–428. DOI: 10.1038/nrc2131
3. Moreno Bueno, G.; Portillo, F.; Cano, A. Transcriptional Regulation of Cell Polarity in EMT and Cancer. *Oncogene* **2008**, *27*, 6958–6969. DOI: 10.1038/onc.2008.346
4. Derynck, R.; Zhang, Y. E. Smad Dependent and Smad Independent Pathways in TGF- β Family Signalling. *Nature* **2003**, *425*, 577–584. DOI: 10.1038/nature02006
5. Tzavlaki, K.; Moustakas, A. TGF-β Signaling. *Biomolecules* **2020**, *10*, 487. DOI: 10.3390/biom10030487
6. Fusco, A.; Fedele, M. Roles of HMGA Proteins in Cancer. *Nat. Rev. Cancer* **2007**, *7*, 899–910. DOI: 10.1038/nrc2271
7. Heimsath, E.; Wood, A. High-Throughput Methods to Quantitatively Evaluate TGF-β Signaling in Epithelial-to-Mesenchymal Transition. Agilent Technologies Application Note **2024**, publication number 5994-6709EN. https://www.agilent.com/cs/library/applications/an-high-throughput-methods-TGF-%CE%B2-signaling-epithelial-5994-6709EN-agilent.pdf
8. Stringer, C.; Wang, T.; Michaelos, M.; Pachitariu, M. Cellpose: A Generalist Algorithm for Cellular Segmentation. *Nat. Methods* **2021**, *18*, 100–106. DOI: 10.1038/s41592-020-01018-x
9. Pachitariu, M.; Rariden, M.; Stringer, C. Cellpose-SAM: Superhuman Generalization for Cellular Segmentation. *bioRxiv* **2025**, 2025.04.28.651001. DOI: 10.1101/2025.04.28.651001

Products used in this application

Agilent products

BioTek Cytation C10 Confocal Imaging Reader

BioTek Gen5 Software for Imaging & Microscopy

www.agilent.com/lifesciences/biotek

PR7005-2358

Published in the USA, September 11, 2026
5994-9387EN

Agilent